QUANTITATIVE LIFETIME MEASUREMENTS WITH PHOTOLUMINESCENCE IMAGING

Manuel The[1], Martin C. Schubert[2], Wilhelm Warta[1]
[1] Fraunhofer Institute for Solar Energy Systems (ISE); [2] Freiburger Materials Research Center University Freiburg
[1] Heidenhofstr.2, 79110 Freiburg, Germany; [2] Stefan-Meier-Str.21, 79104 Freiburg, Germany

ABSTRACT: The measurement of the effective carrier lifetime in silicon has a high importance for the material characterization in the field of photovoltaics since carrier lifetime represents a central quality factor in solar cell production. Photoluminescence has recently evolved as a fast measurement technique for the determination of the minority carrier lifetime in silicon wafers. While PL images of relative values are already available, up to now suitable calibration methods for absolute lifetime values have been developed only for measurements with low spatial resolution. In this paper we propose two different calibration methods for Photoluminescence Imaging measurements with a high spatial resolution: (i) A self consistent calibration procedure is applied to PLI measurements. (ii) We demonstrate a method calibrating relative values of PLI by comparison with a CDI lifetime measurement. The second calibration method accounts for the non-linearity of the PLI signal with lifetime as well as for reabsorption effects.

1 INTRODUCTION

Photoluminescence Imaging (PLI) is a fast and powerful technique for the qualitative determination of the material quality of silicon wafers. Up to now quantitative lifetime images could only be obtained by calibrating each sample with another lifetime measurement technique, and averaging the pixels over a large area [1], [2]. In the following, we demonstrate that a self consistent calibration method, which was recently introduced by T.Trupke et al. for photoluminescence measurements without spatial resolution [3], can also be applied for PLI. Thereby the measured photoluminescence signals can be converted into an absolute excess carrier concentration by the determination of a scaling factor A_i. We also present an easily applicable calibration method, by which the theoretical PL signal is calculated, considering photon reabsorption, and then compared to a different spatially resolved lifetime technique (Carrier Density Imaging CDI, also termed Infrared Lifetime Mapping ILM). The resultant experimental calibration factor K_{cal} allows the calculation of a quantitative recombination lifetime image from a PLI measurement.

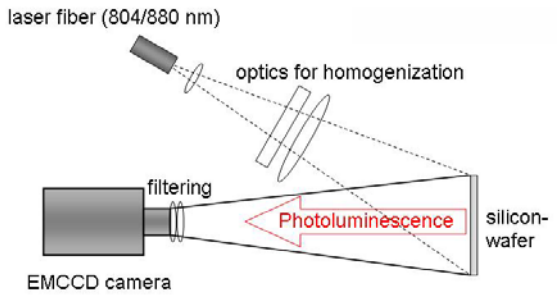

Figure 1: PLI measurement setup. The detection of the photoluminescence spectrum occurs from the front side with an Electron-Multiplying CCD camera (EMCCD)

The PLI setup at ISE Freiburg is shown in Fig. 1. Free excess carriers are generated optionally by a homogeneous laser irradiation with 804 or 880 nm. The 880 nm laser can be modulated arbitrarily. The measurements are taken under room temperature whereas the sample can be placed on a mirror or are free standing. The emitted photoluminescence radiation is detected from the front side by a silicon EMCCD camera. To suppress laser reflections falling into the optical aperture of the camera, a set of long-pass filters is mounted in front of the lens of the camera.

2 SELFCONSISTENT CALIBRATION

With the selfconsistent calibration relative photoluminescence signals can be transformed into absolute excess carrier concentrations and effective lifetimes [3]. The aim of this calibration method is the correct determination of the scaling factor A_i from the luminescence equation (1):

$$I_{PL} = A_i \cdot B \cdot \Delta n \cdot \left(\Delta n + N_A\right). \qquad (1)$$

where B is the radiative recombination coefficient and N_A is the doping density for a p-type wafer. For that purpose the choice of a suitable generation modulation with a rising and falling branch is an important requirement. Since the time dependent excess carrier concentration $\Delta n(t)$ is phase shifted compared to the generation modulation $G(t)$, the influence of the transient behavior for both, rising and falling branch of a generation light is different [see Fig. 2]. In the case of an incorrect choice of A_i hysteresis effects appear in the injection-dependent lifetime data $\tau_{eff}(\Delta n)$ [3]. These hysteresis effects may be described by the differential equation

$$\frac{d\Delta n(t)}{dt} = G(t) - \frac{\Delta n(t)}{\tau_{eff}\left[\Delta n(t)\right]} \qquad (2)$$

and the resultant effective lifetime, by

$$\tau_{eff} = \frac{\Delta n(t)}{G(t) - \frac{d\Delta n(t)}{dt}} = \frac{-\frac{N_A}{2} + \sqrt{\frac{N_A^2}{4} + \frac{I_{PL}}{A_i \cdot B}}}{G(t) - \frac{d\Delta n(t)}{dt}}. \qquad (3)$$

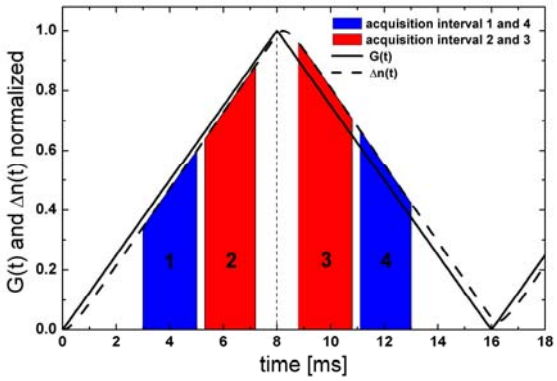

Figure 2: Time dependent excess carrier concentration $\Delta n(t)$ (dashed line) for a triangular generation modulation $G(t)$ (solid line). The acquisition intervals of the camera (blue and red areas) are positioned symmetrically to $G(t)$.

The PL-camera integrates across the acquisition interval positioned symmetrically to the maximum of the generation modulation. Since the camera has a restricted minimum integration time, it is not possible to pick up a large amount of measurements along the rising and falling branch of the generation light as was done in [3]. According to the choice of frequency of $G(t)$ in our case for application to PL-Imaging two measurements per branch are usable. To illustrate that significant hysteresis effects appear in the injection dependent lifetime data even if only four data points per period are recorded, a numerical simulation was performed. For this purpose a triangular generation modulation with peak intensity of $2.5 \cdot 10^{17}$ $cm^{-3}s^{-1}$ and frequency 62.5 Hz was used. A doping density of $N_A = 1.051 \cdot 10^{16}$ cm^{-3} is assumed. If a linear dependence of the effective lifetime τ_{eff} on the injection level Δn is assumed, the excess carrier profile $\Delta n(t)$ can be calculated from the differential equation (2). With an exposure time of 2 ms and $A_i = 1$ an absolute PL-signal was simulated from equation (1) for each data acquisiton interval (see Fig. 2, 1 - 4). This PL-signal can then be used for the calculation of the injection dependent lifetime, according to equation (3), for various scaling factors A_i. The numerically simulated data in Figure 3 demonstrates, that the corresponding injection dependent lifetimes determined in the acquisition

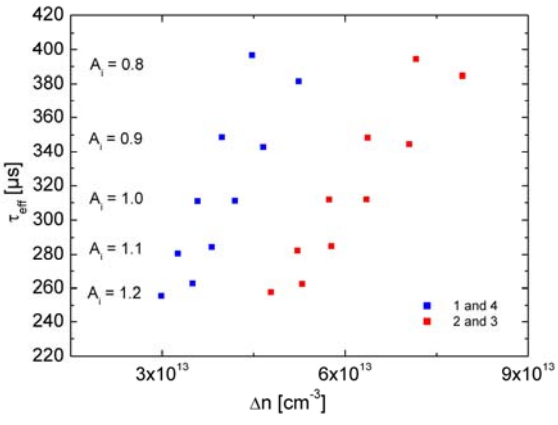

Figure 3: Numerically simulated injection dependent lifetime data for accumulation periods 1 and 4 (blue) and 2 and 3 (red) respectively for various scaling factors

intervals of rising and falling branches diverge for incorrect scaling factors. These hysteresis effects are minimal for $A_i = 1$, resulting in the linear dependence of τ_{eff} and Δn, which was initially implemented in the simulation

Generally, for experimental data, the distinction between a correct and an incorrect scaling factor is not as clear as it is demonstrated in the case of this simulation, because each sample area can have a different injection dependent lifetime characteristic. Therefore additional criteria for the progression of the four injection dependent lifetime data points have to be established. Since PLI is independent of trapping effects under low level injection conditions [4] and all measurements were not performed under high level injection, (i.e Auger recombination is negligible) the effective lifetime has always to increase with injection level or stay constant. Thus the injection dependent lifetime data points derived from the four acquisition intervals must have the following order: $\tau_{eff}(\Delta n_3) \geq \tau_{eff}(\Delta n_2) \geq \tau_{eff}(\Delta n_4) \geq \tau_{eff}(\Delta n_1)$ with $\Delta n_3 > \Delta n_2 > \Delta n_4 > \Delta n_1$. If M_{14}, M_{42}, M_{23} represent the slope between the lifetime data $\tau_{eff}(\Delta n_1)$ and $\tau_{eff}(\Delta n_4)$, $\tau_{eff}(\Delta n_4)$ and $\tau_{eff}(\Delta n_2)$, $\tau_{eff}(\Delta n_2)$ and $\tau_{eff}(\Delta n_3)$, respectively, the latter condition yields always positive slopes.

a)

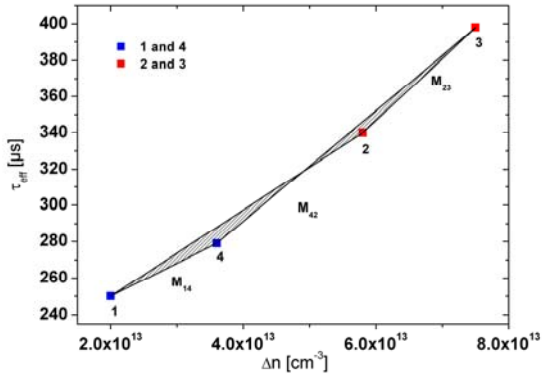

b)

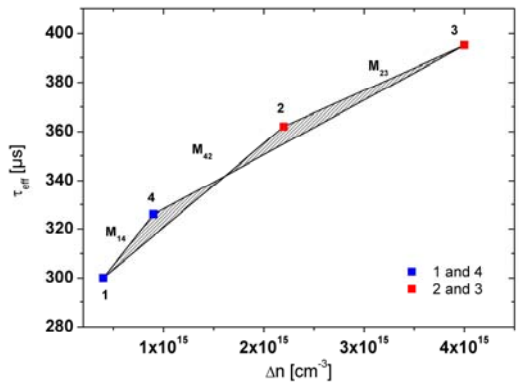

Figure 4: Examples for the progression of the four lifetime data points, which satisfies the criteria for the slopes:
a) $M_{14} \leq M_{42} \leq M_{23}$ and b) $M_{14} \geq M_{42} \geq M_{23}$. The minimization of the area (grey area) included by the experimental lifetime data corresponds to the minimization of the hysteresis effects and yields the correct scaling factor A_i

Beside this main criterium, statements about the order of

these slopes can be made:

1) $M_{14} \leq M_{42} \leq M_{23}$
2) $M_{14} \geq M_{42} \geq M_{23}$

The first case describes the beginning of the Shockley-Read-Hall (SRH) dominated lifetime region, where the slope of the effective lifetime curve increases with the injection level. For the limit of the SRH-dominated lifetime region case 2 holds. The effective lifetime tends towards a maximum. The marginal case of 1) and 2) describes the linear dependence of τ_{eff} and Δn.
All scaling factors which can not satisfy the main criteria or the order of the slopes (1) - 2)) are eliminated from further considerations. To minimize the arising hysteresis effects a minimization of the area, depicted in Figure 4, is proposed. The included area is a function of the scaling factor A_i.
For PLI measurements performed under quasi steady state conditions, where $G(t)$ is constant over the hole measurement range, a lifetime image $\tau_{eff}(x,y)$ can be calculated with the determined scaling factor if the doping density is known:

$$\tau_{eff}(x,y) = \frac{-\frac{N_A}{2} + \sqrt{\frac{N_A^2}{4} + \frac{I_{PL}(x,y)}{A_i \cdot B}}}{G(t)}. \qquad (4)$$

The self consistent calibration method has been applied to PLI measurements on a 1 Ωcm p-type multicrystalline silicon sample with a SiN passivated surface. A fiber coupled laser diode with 880 nm was used for the triangular modulation of the generation light. The frequency of the modulation was set to 62.5 Hz and the peak amplitude corresponding to an absolute generation rate of $2.16 \cdot 10^{17}$ $cm^{-2}s^{-1}$. The incident light intensity was measured with a calibrated Si solar cell. With an exposure time of 2 ms the camera takes four lifetime images in the acquisition interval as described in the section above. An enhancement of the signal to noise ratio could be achieved by averaging over 200 images, which is essential for such a short exposure time. Four injection dependent lifetime data points for various scaling factors could be calculated from the averaged PL signal of each image. An algorithm was developed searching for the right scaling factor by minimization of the included area which is consequently a function of A_i.
In Figure 5a the self-consistently calibrated PL lifetime image of the multycristalline wafer is displayed.
For comparison the absolute values of lifetimes a CDI reference measurement of the same wafer is displayed in Figure 5b. Generally the lifetimes from PL are smaller than the ones from CDI except for the regions of low lifetimes.

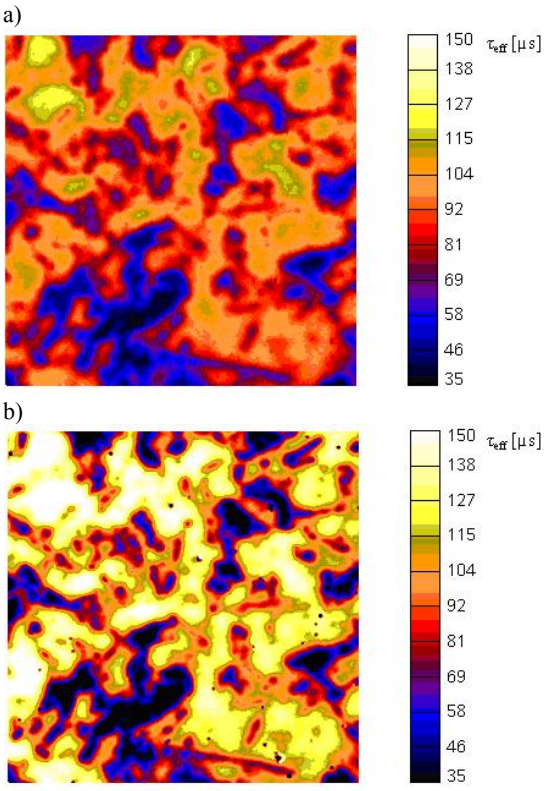

Figure 5: Self consistent calibrated PL lifetime image of a 50 x 50 mm^2 multycristalline wafer (a), and for comparison a CDI lifetime measurement of the same wafer (b).

3 CALIBRATION WITH CDI

Another possibility to obtain a quantitative lifetime image can be provided by calibrating with a different lifetime technique. As a spatially resolved lifetime technique, in particular Carrier Density Imaging (CDI) [5] is available at ISE for the calibration of PLI measurements. The correlation between these two lifetime techniques depends on doping density and thickness of the sample under test. The impact of photon reabsorption on the measured PL-signal varies with these parameters and is strongly dependent on wavelength. While the long wavelength part of the photon emission spectrum depends only weakly on reabsorption, the short wavelength part is significantly affected by reabsorption, due to the absorption coefficient rising with the photon energy [6]. For integral photoluminescence measurements in many cases reabsorption is of minor importance as has been shown recently [7], where a thick silicon detector with reasonable quantum efficiency around 1000 nm is used. For Photoluminescence Imaging, however, reabsorption becomes more important because a Si CCD chip is used where the quantum efficiency above 1000 nm is comparatively low. In contrast to the real photoluminescence spectrum, the center of the detected spectrum is then shifted towards shorter wavelengths, where reabsorption is significant. For a correct calibration reabsorption effects have to be considered. The expected camera signal for PLI can be calculated by

$$I_{PL} = K_{cal} \int_{\lambda_{min}}^{\lambda_{max}} \eta_{camera}(\lambda) T_{filter}(\lambda) dj_0(\lambda) \times \int_{z=0}^{d} \left(\Delta n^2(z) + \Delta n(z) N_A\right) \exp(-\alpha(\lambda) z) dz d\lambda \qquad (5)$$

where K_{cal} is a calibration factor, including the experimental setup geometry e.g camera distance and aperture. K_{cal} has to be determined only once by comparison to a CDI measurement, as will be described in the following section. η_{camera} is the external quantum efficiency of the camera sensor, T_{filter} the transmission of the long-pass filters, j_0 is the band-to-band luminescence spectrum for charge carriers, placed in the distance $z = 0$ from the front side of the wafer with thickness d, and $\alpha(\lambda)$ is the absorption coefficient for silicon. Since free carrier absorption is negligible in the wavelength range of photoluminescence, the total absorption coefficient $\alpha(\lambda)$ is assumed to equal the absorption coefficient for band to band transition $\alpha_{BB}(\lambda)$.

Simulations have been performed to calculate the expected camera signal. For 1.25 Ωcm p-typ wafers with different thickness and a bulk lifetime range similar to the experimentally observed data that will be discussed later, excess carrier concentration Δn(z) have been calculated with PC1D. SiN-passivated surfaces with a surface recombination velocity of S = 10 cm/s and a constant Shockley-Read-Hall lifetime have been assumed. A 804 nm light source was selected with a incident photon flux of $1.79 \cdot 10^{17}$ $cm^{-2}s^{-1}$ which is equivalent to 0.8 suns and corresponds to the experimental conditions. With equation (5) the expected PLI camera signal was calculated with and without reabsorption. The simulation in Fig. 6 shows the influence of surface recombination and reabsorption effects.

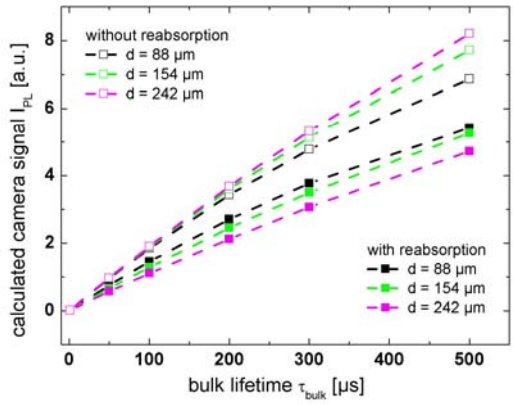

Figure 6: Simulated dependence of the PLI camera signal on bulk lifetime for three different wafer thicknesses with (interior symbols) and without (full symbols) consideration of reabsorption, assuming S = 10 cm/s and a doping density of $N_A = 1.189 \cdot 10^{16}\,cm^{-3}$

Three main effects are detectable: (i) the thicker the sample the higher the impact of reabsorption as exspected, (ii) with decreasing bulk lifetime and thus decreasing diffusion length of the free minority carriers the influence of reabsorption also becomes smaller, (iii) the thinner the sample the higher the impact of surface recombination.

The bulk lifetimes from the simulation in Figure 6 were transformed into effective lifetimes by using the following approach:

$$\frac{1}{\tau_{eff}} = \frac{1}{\tau_{bulk}} + \frac{2S}{d} \quad \text{for} \quad \frac{S \cdot d}{D_n} < \frac{1}{4}, \qquad (6)$$

where D_n is the diffusion constant for the minority carriers. The limitation of validity in equation (6) is fulfilled for S = 10 cm/s and the range of the wafer thickness used. The expected dependence of the PLI camera signal on the effective lifetime, considering reabsorption is shown in Figure 7 (upper graph). If τ_{eff} is assumed to be proportional to Δn over the injection level range under consideration, the simulated data points can be fitted by the non-linear dependence of the PLI camera signal on effective lifetime, resulting in two fitting parameters a_{sim} and b_{sim}:

$$I_{PL,sim} = a_{sim} \cdot \tau_{eff}^2 + b_{sim} \cdot \tau_{eff} \qquad (7)$$

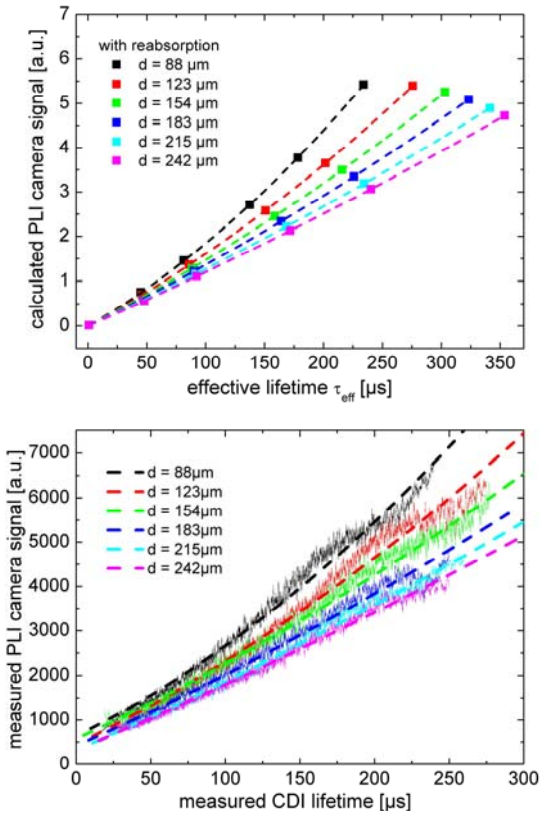

Figure 7: Simulated dependence of the PLI camera signal on the effective lifetime (above) for different wafer thicknesses. The experimentally obtained PLI camera signals versus the effective lifetimes from the CDI measurement (bottom) were fitted according to eq. (8) for each sample (dotted lines). For better illustration a moving average for every pixel curve was performed.

In order to verify these simulations, PLI measurements under steady state conditions have been performed on adjacent multicrystalline 1.25 Ωcm p-type wafers of different thickness. The size of the wafers is 100 x 100 mm^2 and the exposure time for these measurements was 0.5 s only. The surface recombination velocity of the SiN- passivated wafers is estimated to be close to 10 cm/s. These measurements have been compared to recombination lifetime measurements with Carrier

Density Imaging (CDI). After a matching procedure to align images, the PLI signal is plotted versus the effective lifetime data of the CDI pixel by pixel.
In order to allow an easy comparison of the resulting pixel curves for the different wafer thicknesses a moving average over 100 data points was carried out (see Figure 7 bottom). Additionally to the fitting parameters a_{sim} and b_{sim} from the simulated data, a calibration factor K_{cal} and an offset c, which accounts for an additive signal caused by reflections of the generation light, have been fitted for each sample:

$$I_{PL,\exp} = K_{cal} \cdot \left(a_{sim}\tau_{eff}^2 + b_{sim}\tau_{eff}\right) + c \qquad (8)$$

The experimental data shows good agreement with the simulation for the whole lifetime range and all available thicknesses. The resultant parameter K_{cal} should be approximately the same for all wafer thicknesses, because it only depends on the experimental setup. In Table 1 the obtained fitting parameters K_{cal} and c are given for the different wafers. A low relative standard deviation of 4 % confirms the good results for $K_{cal.}$
An average calibration factor and offset c could be extracted from the experimental data for the present setup.
The model description of the PLI signal in combination with the experimental determination of the calibration factor K_{cal} by comparison to a different lifetime technique enable the calculation of a quantitative recombination lifetime image from a PLI measurement.

$$\tau_{eff}(x,y) = -\frac{b_{sim}}{2a_{sim}} + \sqrt{\left(\frac{b_{sim}}{2a_{sim}}\right)^2 + \frac{I_{PL,\exp}(x,y) - c}{a_{sim}K_{cal}}} \qquad (9)$$

For the calculation, the base doping concentration, the thickness and the surface recombination has to be known.

Table I: Fitting parameters for different wafer thickness

wafer thickness d [µm]	K_{cal}	c
88	$1.09 \cdot 10^{-19}$	643
123	$1.16 \cdot 10^{-19}$	449
154	$1.15 \cdot 10^{-19}$	578
183	$1.17 \cdot 10^{-19}$	418
215	$1.22 \cdot 10^{-19}$	319
242	$1.23 \cdot 10^{-19}$	322

An application example of this calibration method is demonstrated in Figure 8. A multycristalline wafer with a thickness of 295 µm, a base doping concentration of N_A = 1.465 · 10^{16} cm^{-3} and an estimated surface recombination velocity of S = 10 cm/s has been measured with PLI and calibrated with respect to equation (9) (Fig. 8 above). An independently calibrated lifetime image measured by the CDI on the same wafer under identical illumination conditions is displayed at the bottom of Figure 8. The averaged lifetime for the PLI measurement is 73 µs, the average of the CDI recombination lifetime is 84 µs. A good quantitative and qualitative agreement is observed between the PL lifetime image and the CDI measurement.

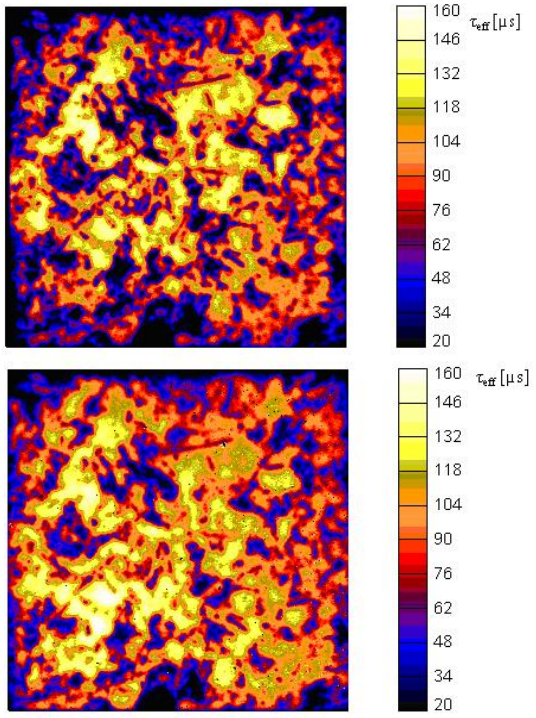

Figure 8: PL lifetime image of a multicrystalline wafer with a SiN passivated surface, calibrated according to eq. (9) (above), and reference measurement with CDI (bottom).

4 CONCLUSION

Quantitative results for PLI are an important step for the industrial implementation of this fast and powerful lifetime technique. In this paper we demonstrated two different calibration methods which enable a quantitative determination of the spatially resolved effective lifetime: (i) A self consistent calibration was applied to a PLI measurement, which converts the relative measured PL signal into an absolute excess carrier density and thus in an effective lifetime. (ii) Simulations have shown that photon reabsorption can have a big impact on the PLI measurement. By considering these reabsorption effects and the non linearity of the PLI signal with lifetime, a generally applicable calibration factor could be determined by the experimental comparison of PLI and CDI.
An advantage of the self consistent method is that no other lifetime technique is required. Due to the small exposure time of 2 ms for samples with a low effective lifetimes the transient effects between two lifetime images used for the calibration could be in the same order of magnitude as the noise of the camera. Then a correct determination of the scaling factor is not possible anymore.
Such sensitivity problems do not appear for the second calibration method, because a higher exposure time can be selected. While the self consistent procedure has to be applied to each sample under test, because the scaling factor depends on the sample properties, the calibration

with CDI has to be performed only several times, if different experimental setups are used, e.g change of distance between camera and wafer, and if the surface condition is different.

ACKNOWLEDGMENTS

The authors would like to thank D. Kray, H. Habenicht H. Lautenschlager and A. Leimenstoll for sample preparation and F. Heinz for measurements. This work was supported by the German Federal Ministry of Education and Research (BMBF) under contract number 01SF0401 ("Netz Diagnostik") and the German Ministry for the Environment, Nature Conservation and Nuclear Safety (BMU) under contract number 0327610A ("SIC-PASS").

References

[1] T. Trupke, R.A. Bardos, M.C. Schubert, W. Warta, Applied Physics Letter, Vol.89, no.4, pp. 44107-1-3, (2006)

[2] T. Trupke, R.A. Bardos, M.D.Abbott, F.W. Chen, J.E. Cotter, IEEE 4th World Conference on Photovoltaic Energy Conversion, 2006, pp.4 Piscataway, NJ, USA

[3] T. Trupke, R.A. Bardos, M.D.Abbott, Applied Physics Letter, Vol 87, 184 (2005)

[4] R. Bardos, T. Trupke, M.C. Schubert, T. Roth, Applied Physics Letter, Vol 88, 53 (2006)

[5] S. Riepe, J. Isenberg, C. Ballif, S.W. Glunz, and W. Warta, 17th EUPVSEC Munich, 2001

[6] M.J. Keevers, M.A. Green, Applied Physics Letter, Vol.66, 174 (1995)

[7] T. Trupke, Journal of applied physics, Vol.100, 6, 63531-1-8 (2006)